Science of the Total Environment 658 (2019) 122–131

Contents lists available at ScienceDirect

Science of the Total Environment

journal homepage: www.elsevier.com/locate/scitotenv

Natural radioactivity in algae arrivals on the Canary coast and dosimetry assessment

A. Tejera *, L. Pérez-Sánchez, G. Guerra, A.C. Arriola-Velásquez, H. Alonso, M.A. Arnedo, G. Rubiano, P. Martel

Physics Department, Universidad de Las Palmas de Gran Canaria, 35017 Las Palmas de Gran Canaria, Spain

HIGHLIGHTS

- Use of wild and cultured seaweed in food industry is increasingly a productive sector.
- Radionuclides bioaccumulation studied in seaweed collected in Canary coast arrivals
- Higher accumulation for marine reactive-particle radionuclides than conservative ones
- ^{210}Po main contributor to the ACED (60% – 85%)
- An internal dose assessment before human consumption of products is advisable.

GRAPHICAL ABSTRACT

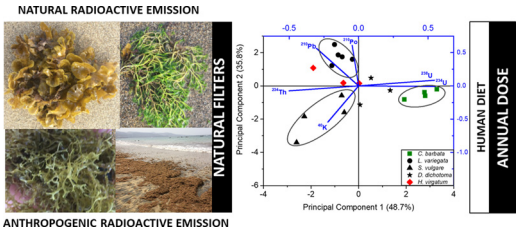

ARTICLE INFO

Article history:
Received 11 September 2018
Received in revised form 7 December 2018
Accepted 10 December 2018
Available online 12 December 2018

Editor: Mae Mae Sexauer Gustin

Keywords:
Seaweed
Natural radionuclides
Concentration factors
Internal dose
Canary Islands

ABSTRACT

Nowadays, the use of wild and culture harvest seaweed in food industry is a booming productive sector. In this context, a radiological characterization of five globally common seaweed species that were collected in arrival on Gran Canaria coast was carried out. The studied algae species were *Cymopolia barbata*, *Lobophora variegata*, *Sargassum vulgare*, *Dictyota dichotoma* and *Haliptilon virgatum*. Radionuclides analysed by alpha and gamma spectrometry were ^{238}U, ^{234}U, ^{235}U, ^{210}Po, ^{234}Th, ^{226}Ra, ^{210}Pb, ^{228}Th, ^{224}Ra, ^{40}K and ^{7}Be. Activity concentrations, ratios, and concentration factors (CF) were determined for all samples collected. The CF in algae was higher for reactive-particle radionuclides (^{210}Po, ^{234}Th, ^{228}Th and ^{210}Pb) than for conservative ones (^{40}K and the uranium isotopes). ^{210}Po, ^{228}Th and ^{234}Th CF were one or two orders of magnitude higher than those recommended by the IAEA. *L. variegata, C. barbata* and *S. vulgare* showed a clear preference for ^{210}Pb and ^{210}Po, for uranium radioisotopes, and for ^{40}K and ^{234}Th, respectively. A dosimetry assessment due to seaweed ingestion showed considerable values of annual committed effective dose for *H. virgatum* (605 ± 19 μSv/y), *L. variegata* (574 ± 17 μSv/y) and *D. dichotoma* (540 ± 30 μSv/y). Hence, this study suggests that an algae radiological characterization is recommended as part of the product valorising process.

1. Introduction

During recent years there has been increased interest in knowledge of the concentration and distribution of natural radionuclides in the marine environment, not only to provide useful information for monitoring environmental radioactivity, but also to assess the radiation risk for marine biota and seafood consumers. Likewise, the transport of radionuclides associated with biological material is not only subject to physical and geological movements, but also to a variety of processes such as bioaccumulation (Faganeli et al., 2017; Uddin et al., 2017), passive sinking of detritus (Cochran et al., 1990), food-chain transfer

* Corresponding author.
E-mail address: alicia.tejera@ulpgc.es (A. Tejera).

https://doi.org/10.1016/j.scitotenv.2018.12.140
0048-9697/

(Pentreath, 1988) and horizontal and vertical migration of many species (Livingston, 2004).

Distribution of radionuclides from the ^{238}U series (^{226}Ra, ^{210}Pb and ^{210}Po) has been well studied in the marine environment. ^{226}Ra tends to be mobilized in seawater whereas its progeny, ^{210}Pb and ^{210}Po, tend to be accumulated by marine biota (McDonald et al., 1992), even with a higher preference for accumulation of ^{210}Po relative to ^{210}Pb in brown algae (Al-Masri et al., 2003; Sirelkhatim et al., 2008). In this way, ^{210}Po is the primary contributor to the natural radiation dose (Mat Çatal et al., 2012). Concentration factors for ^{210}Po have been established in brown algae (*Sargassum*) in the northern Gulf of Kuwait, with values higher than recommended by the IAEA (Uddin et al., 2015). These macroalgae concentrate the radionuclides, and then they can be easily passed along to a higher trophic level of the marine food chain. Therefore, the marine biota can be considered as a potential bioindicator of radionuclides present in its surrounding marine environment (Khan and Wesley, 2016). Regarding the ability of marine organisms (such as ascidians, barnacles, mussels and brown algae) to biomagnify and bioaccumulate radionuclides such as ^{7}Be, ^{234}Th and ^{228}Ra, Ishikawa et al. (2004) have also suggested their role as biological monitors of natural radionuclides in the marine environment. Accordingly, this capacity of macroalgae to accumulate radioisotopes makes it possible to treat them as biological indicators of pollutants in the marine environment (Chakraborty et al., 2014).

Traditionally, seaweed has been used for human consumption, mainly in Asia (Japan, China and Korea). In recent years, an increasing interest in eating seaweed as "sea vegetables" in the west, based on their nutritional or medicinal properties has been reported (Tiwari and Troy, 2015). According to the world review by FAO (2018), in 2016 about 31 million tonnes (fresh weight) of algae were harvested in the world fundamentally for direct human consumption, this production is more than twice that of 2005. However, risks for the human health related to the accumulation of some potential hazardous components in the seaweeds (allergens, toxins, pathogens, potentially toxic trace metals, or radionuclides) have to be assessed (van der Spiegel et al., 2013).

In order to evaluate the risks that are associated with algae intakes, radiological hazard indicators have been reported. In this context, Praveen Pole et al. (2017) calculated the total dose rate of ^{210}Po in several macroalgae species located close to nuclear installations on the southeast coast of India, obtaining values a few orders of magnitude lower than the limits proposed for marine biota (UNSCEAR, 2008). Also, in the Gulf area and the Qingdao coast of China, the radiological hazard index values for the marine biota samples in a study on ^{137}Cs, ^{40}K, ^{226}Ra, ^{228}Ra and ^{238}U reported by Al-Qaradawi et al. (2015) and Yang et al. (2015) were below the levels recommended by the IAEA (1992 and 2014), and there is no impact on human health for seafood consumers.

In this study, radionuclide levels in five algae species, frequently found in canary coast (Gallardo et al., 2016; Guiry, 2018), collected from algae arrivals on Las Canteras beach, were analysed. Alpha and gamma spectrometry techniques were used to measure ^{238}U, ^{234}U, ^{235}U, ^{210}Po, ^{234}Th, ^{226}Ra, ^{210}Pb, ^{228}Th, ^{224}Ra, ^{40}K and ^{7}Be activity concentrations. In order to establish a radiological characterization of algae and explore their use as surrounding environmental tracers, concentration factors and the ratios between the uranium series and uranium/thorium series were determined, and principal component analysis was done. Finally, an assessment of doses due to intakes of radionuclides accumulated by algae was made.

2. Study region

The Canary Islands are located in the northeastern part of the central Atlantic Ocean, southwest of Spain, northwest of the African continent (Fig. 1a). Gran Canaria (Fig. 1b) is a volcanic island located in the middle of the one of the largest navigation corridors, with a high traffic of ships that carry all kinds of substances (Sá et al., 2016). Las Canteras beach (Fig. 1c) is one of the most important urban beaches in Spain situated in the capital city of the island (Las Palmas de Gran Canaria). This beach is internationally known for being virtually free of pollutants, reason why it has been bestowed the Blue Flag according to the Foundation for Environmental Education (FEE).

Las Canteras beach has around 3 km of coast and about 60% of it is protected by the presence of a sedimentary bar in the middle of the water, which emerges during low tide. This bar leads to much smaller waves effect in the northern and central archs than southern arch (Fig. 1c), where the sedimentary bar is not present (Medina Santamaría et al., 2006). This beach morphodynamics, as well as the existence of a wide subtidal platform favour the large accumulation of algae on the shores of the beaches, which thrown by the sea after being released naturally from the rocky or sandy substrate (this event is known as arrivals).

These arrivals of seaweed on Las Canteras beach are natural phenomena generally caused by strong waves and storms in the coastal zone. The amount of algae biomass that arrives on the coast of Gran Canaria depends on the strength of the incident waves, the vegetation covers of the affected area at that time of year, and the local oceanographic conditions like currents or tides. Occasionally, the type of swell that produces the arrivals is due to strong storms generated in the North Atlantic that evolve in the proximity of the Canary Archipelago especially in November and March, which even can bring algae from far away (Portillo Hahnefeld, 2008).

In this work, five of the most common algae found in arrivals were collected (*Cymopolia barbata*, *Lobophora variegata*, *Sargassum vulgare*, *Dictyota dichotoma* and *Haliptilon virgatum*). *C. barbata* (Chlorophyta group) is frequent in shallow intertidal tide pools, and in the subsoil sand or rock bottom that covers extensive areas between the bar and the shore of the beach (Espino et al., 2007). *L. variegata* (Phaeophyceae group) is also very common from the intertidal zone to about 30 m deep. It is found on rocky substrate (Espino et al., 2007). *S. vulgare* (Phaeophyceae group) has its natural habitat in firm substrates in the shallow sublittoral zone and arrives on the beach because of strong periods of swell with a west component. Due to their buoyancy capacity, these types of algae reach the coast of the Canary Island Archipelago driven by waves coming from the strong storms in southeastern North America (Espino et al., 2007; Portillo Hahnefeld, 2008). *D. dichotoma* (Phaeophyceae group) is frequently found on the walls of intertidal tide pools and is one of the more abundant species in the Canary Islands (Espino et al., 2007). *H. virgatum* (Rhodophyta group) is found in areas between 0 and 2 m, in tide pools and on intertidal platforms that emerge during low tide (Espino et al., 2007). Finally, these algae are also found in other place as Europe, America, Atlantic, Caribbean, Pacific, and Indian Ocean Islands (Guiry, 2018).

3. Materials and methods

3.1. Sampling and sample preparation

Algae were collected along Las Canteras beach in the intertidal area at low tide for a period of 6 months, from January to June 2017. Algae were washed thoroughly with seawater in situ to remove extraneous sand and debris. Algae were placed in polyethylene containers and brought to the laboratory, where they were immediately oven-dried at 80 °C for 24 h, crushed in a mortar and sieved through 1-mm mesh. Samples were weighed before (fresh weight, FW) and after drying (dry weight, DW). The homogenized samples were deposited into PVC trunk-conical containers and sealed with aluminium strips to minimize radon leakage in gamma spectroscopy analyses.

An aliquot of about 0.5 g of each homogenized sample, previously prepared, was reserved to determine ^{234}U, ^{235}U, ^{238}U and ^{210}Po radionuclides by alpha spectrometry. Algae samples were weighed and spiked with a known amount of ^{209}Po and ^{232}U as tracers. Then they were digested in Savillex Teflon vials in an oven at 80 °C for 48 h (Hierro et al., 2012). When the solutions were totally digested, the dry residue was redissolved in 8 M nitric acid. For isolation of the radionuclides of

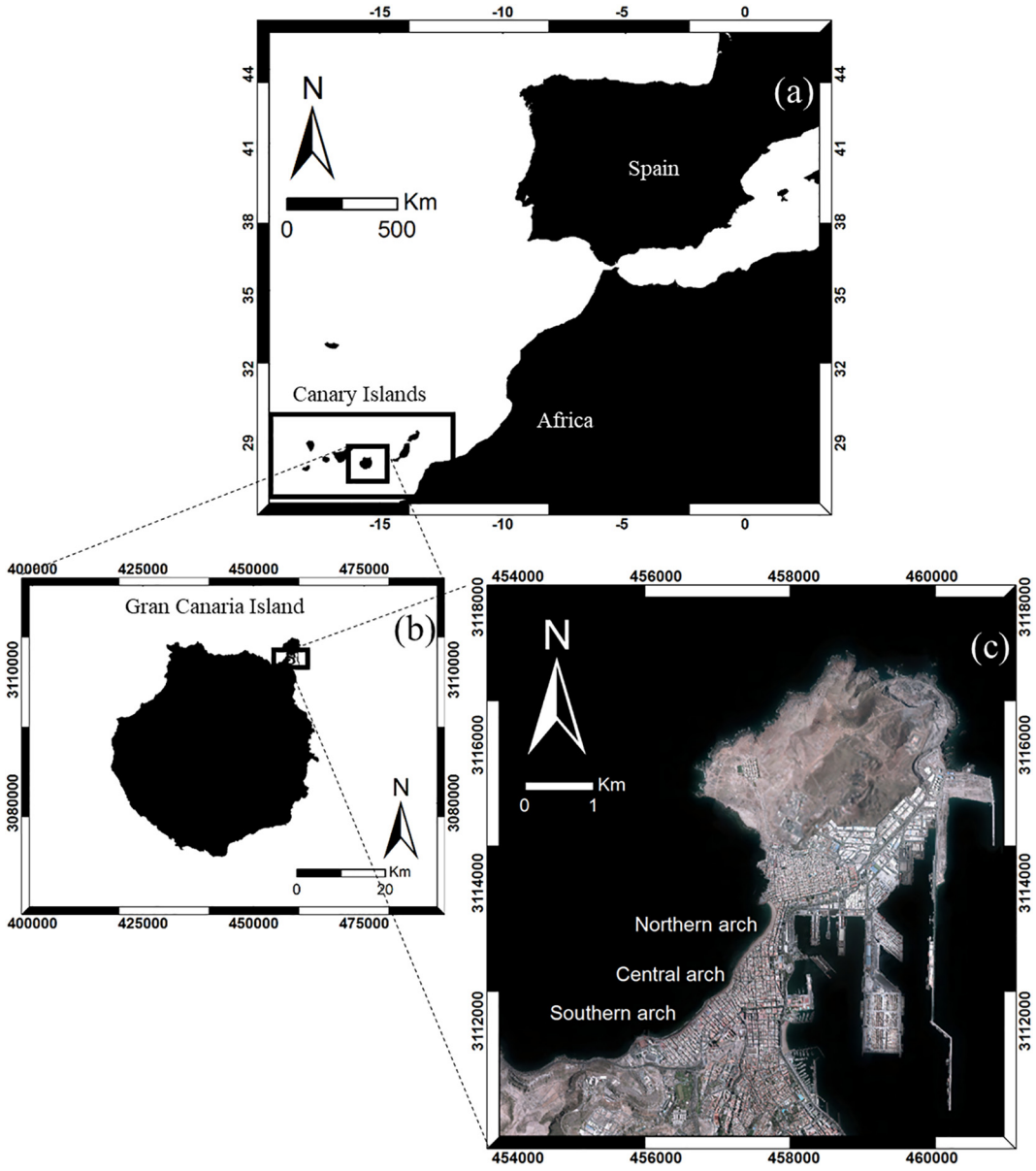

Fig. 1. Location of study zone; a) Canary Archipelago; b) Gran Canaria island; c) Satellite images of Las Canteras beach with its division in archs and Las Palmas port. Coordinates are in the UTM system.

Po and U, a sequential radiochemical method based on an extraction technique with tributyl phosphate (TBP) was applied (Blasco et al., 2016; Bolívar et al., 2000). In this method, once the radionuclides are isolated and purified, Po isotopes are spontaneously plated onto silver discs overnight at room temperature while U isotopes are electrodeposited onto stainless steel discs.

3.2. Gamma and alpha spectrometric analysis

Radionuclides of the ^{238}U series (^{234}Th, ^{226}Ra and ^{210}Pb) and ^{232}Th series (^{228}Ra, ^{228}Th and ^{224}Ra), and non-series radionuclides like ^{40}K and ^{7}Be, were determined by gamma spectrometry. This technique also allows detection of anthropogenic gamma-emitter radionuclides such as ^{137}Cs, ^{241}Am or ^{131}I. For each sample, two gamma measurements were made. A first gamma measurement was made (within 3 and 8 after collection) in order to obtain the activity of short-lived radioisotopes such as ^{7}Be, ^{224}Ra and ^{234}Th. Subsequently, the samples were stored for at least 28 days before the second gamma count to allow secular equilibrium between ^{226}Ra and ^{222}Rn (Arnedo et al., 2013, 2017).

Gamma spectrometric measurements were performed with a CANBERRA Extended Range (XtRa) Germanium spectrometer, model GX3518. This detector has 38% relative efficiency to a 3" × 3" area, and nominal FWHM of 0.875 keV at 122 keV and 1.8 keV at 1.33 MeV, and it works coupled to a CANBERRA DSA-1000 multichannel analyser. Efficiency calibration of the system is carried out using the CANBERRA LabSOCS package based on the Monte Carlo method (Arnedo et al., 2017; G. Guerra et al., 2015, 2017). Calibration was verified using reference standards for IAEA RGK-1, RGU-1 and RGTh-1. Energy calibration was performed using ^{155}Eu/^{22}Na (CANBERRA ISOXSRCE, 7F06-9/10138 series) and confirmed using the 1460.8 keV line of ^{40}K (IAEA RGK-1) (Arnedo et al., 2017).

For each sample, the activity concentrations of ^{234}Th, ^{226}Ra, ^{210}Pb, ^{228}Ra, ^{228}Th, ^{224}Ra, ^{40}K, ^{7}Be and ^{137}Cs were obtained. ^{234}Th was measured through its peak of 63.3 keV. ^{226}Ra was determined from ^{214}Pb using the 351.9 keV emission line. ^{210}Pb was directly determined using the 46.5 keV emission line. ^{228}Ra was determined from ^{228}Ac by the 911.2 keV emission line. Both ^{224}Ra and ^{228}Th were measured from ^{212}Pb by the 238.6 keV emission line (for the above-mentioned first and

second gamma measurement respectively). ^{40}K, ^{7}Be and ^{137}Cs were directly measured, using 1460.8 keV, 477.6 keV and 661.8 keV emission lines, respectively. The counting time for each sample was around 86,700 s. Moreover, due decay corrections were performed so that ^{224}Ra and ^{234}Th activity concentrations are referred to the collection date.

Measurement of alpha radionuclides was performed by ion-implanted silicon detector (PIPS) α-spectrometers (CANBERRA Model PD-450.18 AM) with a 450 mm^2 active area. The counting efficiencies of the detectors were between 21% and 25%. The samples were generally measured about 5 mm from the detector and for 345,600 s, in order to get appropriate minimum detectable activities (MDA) of 0.1 mBq/L (U) and 0.4 mBq/L (Po) (Montaña et al., 2013). For each sample, the activity concentrations of ^{238}U, ^{235}U, ^{234}U and ^{210}Po were obtained by this technique.

Finally, regarding gamma and alpha spectrometry quality assurance, measurements by means of both techniques of reference materials samples with very similar characteristics to those measured in this work (organic matrix) were performed in our laboratory. These reference materials were the IAEA 447 and IAEA 446 which are moss and algae samples respectively. A good accordance was observed among the measuring results and the reference values, confirmed by standard accuracy and precision tests used in IAEA proficiency tests (Shakhashiro et al., 2012; Osvath et al., 2016). Besides, the Canberra ISOCS/LabSOCS, used for gamma spectrometry analyses allows efficiency calibration for a wide range of both measuring geometries (Bronson, 2003) and sample materials including marine biota (Yang et al., 2015).

4. Results and discussion

4.1. Radionuclide concentration

Activity concentrations of the natural radionuclides of the different algae are shown in Table 1. Maximum activity concentrations for ^{238}U and ^{234}U were found for the green alga, *C. barbata*, with mean values of 21.0 ± 1.7 and 29 ± 2 Bq/kg, respectively. The rest of the algae, both brown and red, showed similar means, 11.6 ± 1.2 and 11.7 ± 1.1 Bq/kg, respectively, for ^{238}U and 14.2 ± 1.3 and 14.4 ± 1.3 Bq/kg, respectively, for ^{234}U. The highest values of activity concentrations for ^{235}U were obtained for green algae (with an average value of 2.8 ± 0.4 Bq/kg), and the lowest for the brown group (0.8 ± 0.3 Bq/kg) according to the ^{235}U activities reported for certified reference material IAEA-446 (0.41 ± 0.12 Bq/kg), composed of brown seaweed from the Baltic Sea (Pham et al., 2014).

The high levels of ^{234}U and ^{238}U radioisotopes for green algae found in this work contrast the results given by Burger et al. (2006) and Sakamoto et al. (2008) for algae in the Pacific Ocean, reporting highest activities of both uranium radioisotopes for brown algae and lowest for green algae (Table 2). They explained this result by the adsorptive capacity of the alginic acid present in the cell walls of brown algae. However, the opposite behaviour observed here could indicate a greater dependence on other factors, such as the different biogeochemical and oceanographic properties of each ocean (Atlantic and Pacific), or because different types of green and brown algae were studied.

The mean ^{210}Po activity concentration achieved a maximum value in the brown algae group (156 ± 6 Bq/kg), the highest values being recorded for the species L. *variegata*. Instead, similar values were reported for green and red groups, with averages of 116 ± 5 and 115 ± 4 Bq/kg, respectively (Table 1). These were significantly higher than those determined by other authors (Table 2), even higher than those obtained by El Samad et al. (2014) in brown algae from the coastal environmental surrounding a fertilizer plant (22 Bq/kg FW compared to 30.4 Bq/kg FW obtained in this work). Variations shown for different locations could be due to particulate matter dynamics in each zone, driven by the scavenging of ^{210}Po (Sirelkhatim et al., 2008).

In Table 1, it can be seen that the species L. *variegata* and *H. virgatum* showed maximum mean activity concentrations for ^{210}Pb that were significantly higher than those obtained by other authors (Table 2). *C. barbata* (green algae) exhibited lower values for this radionuclide as well as for ^{234}Th; the latter had rather higher activity concentrations for the rest of the algae, especially for *S. vulgare*. This enrichment of ^{234}Th in *S. vulgare* has been related to adsorption and absorption processes (Ishikawa et al., 2004).

The minimum activity concentration for ^{40}K was obtained in *H. virgatum* (red algae). The values obtained were even lower than those found in the literature for red algae (Table 2). Moreover, ^{7}Be

Table 1
Activity concentration and their mean (Bq/kg DW) of alpha and gamma emission radionuclides for each alga sample and group. DW/FW is ratio between dry and fresh weights.

Sample	DW/FW	^{238}U	^{234}U	^{235}U	^{210}Po	^{234}Th	^{226}Ra	^{210}Pb	^{228}Th	^{224}Ra	^{40}K	^{7}Be
GC1	0.146	14.9 ± 1.2	27.5 ± 1.9	7.0 ± 0.8	116 ± 5	147 ± 12	6.1 ± 1.7	10 ± 6	5.3 ± 1.3	25 ± 3	1020 ± 50	BDL
GC2	0.181	24.3 ± 1.4	26.0 ± 1.5	1.6 ± 0.2	100 ± 4	118 ± 11	9.6 ± 1.9	20 ± 7	12.1 ± 1.5	23 ± 4	1010 ± 50	BDL
GC3	0.209	22 ± 2	33 ± 3	1.2 ± 0.4	129 ± 6	89 ± 8	2.8 ± 1.4	13 ± 5	8.6 ± 1.1	9 ± 3	550 ± 30	BDL
GC4	0.227	23 ± 2	28 ± 2	1.4 ± 0.4	119 ± 6	100 ± 11	18 ± 2	25 ± 7	14.8 ± 1.7	8 ± 2	1160 ± 60	BDL
Mean		**21.0 ± 1.7**	**29 ± 2**	**2.8 ± 0.4**	**116 ± 5**	**110 ± 10**	**9.0 ± 1.8**	**17 ± 6**	**10.2 ± 1.4**	**16 ± 3**	**940 ± 50**	–
BL1	0.157	11.6 ± 1.1	13.2 ± 1.2	0.7 ± 0.3	243 ± 6	520 ± 40	29 ± 2	83 ± 9	20.3 ± 1.8	25 ± 6	420 ± 30	BDL
BL2	0.166	12.4 ± 0.9	16.6 ± 1.1	0.5 ± 0.2	217 ± 5	570 ± 30	21 ± 2	74 ± 8	13.8 ± 1.5	50 ± 4	820 ± 40	BDL
BL3	0.190	9.8 ± 0.8	10.8 ± 0.8	0.5 ± 0.2	195 ± 5	460 ± 30	10.9 ± 1.6	63 ± 7	10.9 ± 1.3	28 ± 3	860 ± 40	BDL
BL4	0.171	13.5 ± 1.0	18.4 ± 1.2	0.5 ± 0.2	182 ± 7	510 ± 30	8.3 ± 1.8	76 ± 8	19.5 ± 1.6	44 ± 5	580 ± 30	BDL
BL5	0.221	12.8 ± 1.9	10.9 ± 1.7	0.9 ± 0.4	223 ± 8	420 ± 30	14 ± 1.8	73 ± 7	12.9 ± 1.4	35 ± 9	790 ± 40	BDL
Mean		**12.0 ± 1.1**	**14.0 ± 1.2**	**0.6 ± 0.2**	**212 ± 6**	**500 ± 30**	**16.7 ± 1.9**	**74 ± 8**	**15.5 ± 1.5**	**37 ± 6**	**690 ± 40**	–
BS1	0.121	7.2 ± 0.7	10.6 ± 0.8	0.5 ± 0.2	120 ± 3	990 ± 80	8.7 ± 1.7	30 ± 8	10.7 ± 1.3	7 ± 3	3040 ± 130	BDL
BS2	0.114	12.8 ± 1.7	15.5 ± 1.9	1.0 ± 0.4	118 ± 5	860 ± 50	17.4 ± 1.9	35 ± 7	5.5 ± 1.3	19 ± 6	1310 ± 60	BDL
BS3	0.108	5.4 ± 0.6	8.1 ± 0.8	0.16 ± 0.10	40.9 ± 1.8	910 ± 50	9.6 ± 1.8	22 ± 7	11.5 ± 1.4	BDL	3920 ± 170	BDL
BS4	0.152	11.3 ± 1.2	13.9 ± 1.3	0.4 ± 0.2	BLD	650 ± 40	18 ± 3	BDL	34 ± 3	BDL	1370 ± 70	BDL
Mean		**9.2 ± 1.0**	**12.0 ± 1.2**	**0.5 ± 0.2**	**93 ± 3**	**860 ± 50**	**13 ± 2**	**29 ± 7**	**15.4 ± 1.7**	**13 ± 4**	**2410 ± 110**	–
BD1	0.317	15.6 ± 1.1	22.5 ± 1.5	0.9 ± 0.2	127 ± 6	164 ± 11	19.0 ± 1.5	29 ± 5	17.4 ± 1.2	31 ± 4	1060 ± 50	BDL
BD2	0.320	15 ± 2	17 ± 2	1.4 ± 0.5	160 ± 11	242 ± 15	12.5 ± 1.3	44 ± 5	18.1 ± 1.2	23 ± 2	940 ± 40	BDL
BD3	0.197	12.3 ± 1.6	12.9 ± 1.6	2.3 ± 0.6	95 ± 5	276 ± 17	12.8 ± 1.4	21 ± 5	9.3 ± 1.0	18 ± 2	1510 ± 70	BDL
Mean		**14.2 ± 1.6**	**17.5 ± 1.8**	**1.5 ± 0.5**	**127 ± 7**	**227 ± 14**	**14.8 ± 1.4**	**31 ± 5**	**15.0 ± 1.1**	**24 ± 3**	**1170 ± 50**	–
Brown mean		**11.6 ± 1.2**	**14.2 ± 1.3**	**0.8 ± 0.3**	**156 ± 6**	**550 ± 40**	**15.1 ± 1.9**	**50 ± 7**	**15.3 ± 1.5**	**28 ± 5**	**1380 ± 60**	–
RH1	0.454	11.5 ± 0.8	13.0 ± 0.9	0.8 ± 0.2	130 ± 3	1300 ± 100	21.0 ± 1.7	76 ± 8	25.1 ± 1.5	BDL	177 ± 16	36 ± 5
RH2	0.216	10.0 ± 1.1	14.0 ± 1.4	0.7 ± 0.3	104 ± 3	510 ± 30	17.6 ± 1.5	53 ± 6	16.2 ± 1.2	14 ± 4	570 ± 30	29 ± 4
RH3	0.251	13.5 ± 1.4	16.1 ± 1.5	1.8 ± 0.4	111 ± 6	540 ± 30	11.9 ± 1.0	43 ± 4	14.0 ± 0.9	30 ± 5	430 ± 20	8 ± 3
Mean		**11.7 ± 1.1**	**14.4 ± 1.3**	**1.1 ± 0.3**	**115 ± 4**	**770 ± 50**	**16.8 ± 1.4**	**57 ± 6**	**18.4 ± 1.2**	**22 ± 5**	**390 ± 20**	**25 ± 4**

BDL: Below detection limit.

Table 2
Comparison of activity concentration in Bq/kg DF of ^{210}Po, ^{226}Ra, ^{40}K, ^{210}Po and ^{235}U in Las Canteras beach with other authors values. [a] are values in Fresh Weigh. G, B and R correspond to Green, Brown and Red, respectively.

Location	Type	^{238}U	^{234}U	^{226}Ra	^{210}Pb	^{210}Po	^{228}Th-^{228}Ac	^{40}K	References
Las Canteras beach (Spain)	G	(14.9–24.3) 21.0	(26.0–33) 29	(2.8–18) 9.0	(10–25) 17	(100–129) 116	(5.3–14.8) 10.2	(550–1160) 940	This work
	B	(5.4–15.6) 11.6	(8.1–22.5) 14.2	(9.6–29) 15.1	(21–83) 50	(40.9–243) 156	(5.5–20.3) 15.3	(420–3920) 1380	
	R	(10.0–13.5) 11.7	(13.0–16.2) 14.4	(11.9–21.0) 16.8	(43–76) 57	(104–130) 115	(14.0–25.1) 18.4	(177–570) 390	
Point Calimere Coast	B				(13.7–95.0) 54.4	(2.8–2.9) 2.6			Suriyanarayanan et al., 2007
Bulgarian Black sea	G			(3−1300)	(3−100)			(370–2500)	Strezov and Nonova, 2009
	B			(2–17)	(2−21)			(130–1990)	
	R			(2–39)	(4–41)			(124–2100)	
Arab Emirates	G			(16.5–18.3) 17.4			(4.4–61.8) 16.2	(100–4444) 1045	Goddar and Jupp, 2002
	B			(19.1–48.2) 25.6			(5.0–106) 26.2	(125–5443) 2049	
	R			(19.1–48.2) 5.1			(1.6–60.8) 15.3	(278–4373) 1643	
Syrian coast	G			<2.3	(2.3–5.6) 3.8	(7.7–15.56) 12.4		(450–1100) 850	Al-Masri et al., 2003
	B			(1.2–6.8) 3.9	(2.8–15.9) 8.1	(8.1–26.4) 19.5		(551–2260) 1523	
	R			<6	(7.8–27.5) 20.4	(19.5–27.4) 22.3		(70–1030) 402	
White Sea (NIST-SRM)	B	8.7	9.5	5.7	21.0	20.6	3.8	734	Outola et al., 2006
Baltic Sea (IAEA-446)	B	9.3	10.5	17.0	10.9	10.9	15.0	660	Pham et al., 2014
Amchirtka and Kiska Islands	G	0.2[a]	0.3[a]						Burger et al., 2006
	B	(0.4–2.7) 1.2[a]	(0.4–3.1) 1.4[a]						
Kuwait	B				(15.3–22.0)	(22.2–25.6)			Uddin et al., 2015
Japan coast	G	(0.6–4.8)	(0.6–4.9)						Sakamoto et al., 2008
	B	(16.1–58.1)	(16.2–58.5)						
	R	(2.8–9.9)	(2.9–10.0)						

was only observed for *H. virgatum*, while in the rest of the algae it was not detected. ^{7}Be is found in the atmosphere (Rajacic et al., 2017). As mentioned in Section 2, *H. virgatum* is found in areas which emerge during low tide, so it is exposed to interaction with the atmosphere and its components while the other algae species always stay underwater. This could be the reason why only these algae have selectivity of absorption for this radionuclide.

Finally, artificial radionuclides were not detected in any samples, so it could be used as an indicator of the absence of anthropogenic radioactivity in the surrounding marine environment.

4.2. Concentration factors

The values of the respective activity concentrations for these radionuclides in marine water (Table 3) have been taken from typical coastal water activities given by Hosseini et al. (2010, 2012). Although the exact location of the algae is not known because we worked with arrivals, some measurements were made with water samples from the shore of the beach, giving similar values for activity concentrations to those referenced for ^{238}U, ^{234}U, ^{235}U, ^{210}Po and ^{40}K. One can see that these values are much lower than the corresponding activity concentration found for algae. In order to give an idea of the accumulation trend of the radionuclides in the different species of algae, the concentration factor (CF) was calculated (Table 3). This is defined by the ratio of the activity concentration of the radionuclide, per unit of FW, of organism tissue to the corresponding activity, per unit of volume, of the seawater. It is a quantitative indicator of the relationship between the organism and its environment (Inoue et al., 2005).

Table 3 shows that the particle-reactive ^{210}Po, ^{234}Th, ^{210}Pb, and ^{228}Th had the highest CF of between 10^3 and 10^4, accumulation being slightly lower in the green algae. On the other hand, accumulation of the conservative ^{238}U, ^{234}U, ^{235}U and ^{40}K was lower, with CF between 10^1 and 10^2. The CF of ^{226}Ra and ^{224}Ra were in the order of 10^2 or 10^3.

Table 3
Concentration factor (L/kg) of the different radionuclides per algae specie. BMean represents the average between the brown algae. Activity concentration of naturally occurring radionuclide in coastal marine water (Bq/L) compiled by Hosseini et al. (2010) are also included.

Nuclide	Activity (in coastal waters)	Green	Brown				Red
		GC	BL	BS	BD	BMean	RH
^{238}U	0.041	1×10^2	5×10^1	3×10^1	1×10^2	6×10^1	9×10^1
^{234}U	0.047	1×10^2	5×10^1	3×10^1	1×10^2	6×10^1	9×10^1
^{235}U	0.0019	2×10^2	6×10^1	3×10^1	2×10^2	9×10^1	2×10^2
^{210}Po	0.002	1×10^4	2×10^4	5×10^3	2×10^4	2×10^4	2×10^4
^{234}Th	0.012	2×10^3	7×10^3	9×10^3	5×10^3	7×10^3	2×10^4
^{226}Ra	0.0034	5×10^2	9×10^2	5×10^2	1×10^3	8×10^2	2×10^3
^{210}Pb	0.002	2×10^3	7×10^3	2×10^3	5×10^3	5×10^3	9×10^3
^{224}Ra(^{228}Ra)[a]	0.01	2×10^2	4×10^2	2×10^2	6×10^2	4×10^2	5×10^2
^{228}Th	0.0003	7×10^3	9×10^3	7×10^3	1×10^4	1×10^4	2×10^4
^{40}K	12	1×10^1	1×10^1	2×10^1	3×10^1	2×10^1	9×10^0

[a] Activity concentration of ^{228}Ra has been considered.

It is noteworthy that the CF obtained for ^{210}Po in all macroalgae in this study was in the order of 10^4, one order greater than the IAEA recommended value for macroalgae (IAEA, 2014), and the same order as found for two *Sargassum* species along the coast of Kuwait (Uddin et al., 2015), and those reported for a large number of green, brown and red algae along the coast near a nuclear installation on the southeast coast of India (Praveen Pole et al., 2017). ^{210}Pb had a CF of the same order as the IAEA recommended value for *C. barbata* and *S. vulgare* and one order higher than for the rest of the algae. With respect to the CF for ^{234}Th and ^{228}Th, all algae presented values one or two orders higher than recommended by the IAEA (10^2) for thorium. Despite this high accumulation, it should be taken into account that ^{234}Th is a short-lived radionuclide (24 days). The accumulating power of ^{226}Ra was also higher than that recommended by the IAEA (2014) for all algae species, especially for *D. dichotoma* and *H. virgatum*. Different authors point out that the accumulation of metals in macroalgae is very variable and is determined by the life cycle, morphology, contact surface area, growth rate, and specific affinity for a selected metal of a particular species (Chakraborty et al., 2014; Kim et al., 2017). Values obtained for uranium radioisotopes were of the same order as those recommended by the IAEA.

Finally, this biomagnification that algae seem to exhibit for particle-reactive (^{210}Po, ^{234}Th, ^{210}Pb and ^{228}Th) against conservative radionuclides (^{238}U, ^{234}U, ^{235}U and ^{40}K) could indicate a greater affinity to concentrate the particulate phase of seawater than dissolved forms. This fact might be due to an enrichment of the algae's habitat in these particle-reactive radionuclides that are removed from the dissolved phase by scavenging and sink in the water column associated with particles containing carbon and nitrogen (such as POC, PIC and PN) (Wei et al., 2011; Waples et al., 2006).

4.3. Uranium and thorium series ratios

Activity concentration ratios and their average values for the ^{238}U series (^{234}Th/^{238}U, ^{234}U/^{238}U, ^{226}Ra/^{238}U, ^{210}Pb/^{226}Ra, ^{210}Po/^{210}Pb), ^{232}Th series (^{224}Ra/^{228}Th), between them (^{228}Th/^{234}Th, ^{224}Ra/^{226}Ra), and between the uranium series (^{235}U/^{238}U) for the algae analysed are shown in Fig. 2 and Table 4, respectively.

The ^{234}Th/^{238}U values presented important deviations from the secular equilibrium, as well as from the typical marine water ratio, mainly for brown and red algae (Fig. 2a). These disequilibria were also considerable for ^{210}Pb/^{226}Ra (Fig. 2d) and ^{210}Po/^{210}Pb (Fig. 2e). These three ratios, used for estimating the export flux of POC, PIC, and PN (Wei et al., 2011), once again indicate the above-mentioned hypothesis about the possible adsorption/absorption of particulate phase enrichened with particle-reactive radionuclides (^{234}Th, ^{210}Pb, ^{210}Po). Concretely the ^{210}Po/^{210}Pb ratios reflect the known marine biota preference for polonium, as well as the different scavenging affinities of ^{210}Po and ^{210}Pb for biogenic and lithogenic particulate matter, based on their different chemical behaviour (Su et al., 2017; Theng et al., 2005; Hu et al., 2014). On the other hand, the ^{226}Ra/^{238}U values obtained were higher than the typical ratios for marine water (Fig. 2c). These measured values are closer to the common ratios for coastal water where submarine discharges occur.

For all the algae species (Fig. 2b), similar ^{234}U/^{238}U ratios were found with respect to those observed for marine water, around 1.3 in algae and 1.2 in oceanic water (Boryło and Skwarzec, 2014). Consequently, the algae do not seem to show selective absorption of these radionuclides, such as ^{40}K, which are considered to have conservative properties for marine water masses. Some researchers (Inoue et al., 2005) have suggested the use of radionuclides as tracers of water masses, specifically for *S. vulgare* that travels a long distance and could be an indicator of the waters from which it is derived. In this sense, the ^{40}K/^{238}U ratio was calculated for *S. vulgare*; we obtained values of 420 ± 40 and 720 ± 90 for samples BS1 and BS3, and 102 ± 14 and 122 ± 14 for BS2 and BS4. This result could reflect that these arrivals have been driven by water from different zones. Also, ^{235}U/^{238}U (Fig. 2h) in all the algae followed a behaviour similar to that of the sea water.

Finally, results obtained for radionuclides of the ^{232}Th series (^{228}Th and ^{224}Ra) exhibited no secular equilibrium (Table 4). In order to compare activity concentrations between the ^{232}Th and ^{238}U series, ^{228}Th/^{234}Th and ^{224}Ra/^{226}Ra ratios were evaluated (Table 4, Fig. 2g–f). *C. barbata* and *D. dichotoma* showed ^{228}Th/^{234}Th ratios slightly over the one for coastal marine waters. Also, in Fig. 2g, a typical ^{228}Ra/^{226}Ra ratio for a coastal zone where discharges are common, and the marine water ^{228}Ra/^{226}Ra ratio, were also plotted. In this figure, ^{224}Ra/^{226}Ra values were found between those for the two ratios mentioned above. This could reflect that most algae are located in coastal water enriched in ^{228}Ra and so also in its progeny, ^{228}Th and ^{224}Ra. In fact, minimum ^{228}Th/^{234}Th and ^{224}Ra/^{226}Ra averages were found for *S. vulgare* (Table 4) that, as indicated, may well come from another ocean water region.

4.4. Statistical analysis

A Kolmogorov–Smirnov test was conducted for each single variable (radionuclides), and we do not reject the null hypothesis of normality ($p < 0.05$). The Pearson correlation matrix of radionuclides was calculated and is summarized in Table 5. ^{7}Be was not considered because only red algae had values above the detection limit. Correlation coefficients were considered statistically significant when $p < 0.05$. Strong positive correlations were observed between ^{234}U and ^{238}U and between ^{210}Pb and ^{210}Po while strong negative correlations were found between ^{234}Th and ^{238}U and ^{234}U. The latter reinforces the idea already mentioned about accumulation of ^{234}Th linked more with its presence in the particulate phase than with a physiological property of algae, which would imply a strong but negative correlation between ^{234}Th and ^{234}U and ^{238}U. Some moderate correlations were also found, positive between ^{210}Pb and ^{226}Ra, ^{224}Ra and ^{210}Po, ^{224}Ra and ^{210}Pb, and negative between ^{40}K and ^{210}Po, ^{228}Th and ^{226}Ra, ^{210}Pb and ^{234}U.

In order to confirm the underlying pattern between the radiological variables (radionuclide activity concentrations) in the different groups of algae and to help the data interpretation, principal component analysis (PCA) was carried out (Thomson and Emery, 2014). PCA transforms the original variables into a new set of variables (principal components) which are linear combinations of the original ones, in such a way that usually the first two or three principal components are able to explain most of the variation of all original variables (Kohler and Luniak, 2005; Matiatos et al., 2014; Tang et al., 2017). The variables taken into account for this analysis were those showing significant differences between groups of algae according to a oneway ANOVA previously carried out. Three principal components were found to explain 92.6% of the data variability, 48.7% by PC1, 35.8% by PC2 and 8.1% by PC3, respectively. The factor loadings obtained for the first four principal components are shown in Table 6, and scores of observations in PC1 and PC2 were plotted using a biplot (Fig. 3). Additionally, considering the cutpoints of a perpendicular from each observation to different variable lines of the multivariant space of the original variables (radiological variables), three clusters were detected in the biplot (Fig. 3). The clusters formed by *L. variegata* had a clear preference for ^{210}Pb and ^{210}Po, the *C. barbata* group for uranium radioisotopes, and the *S. vulgare* set for ^{40}K and ^{234}Th. Identical clusters are observed when PCA is performed considering all variables used in the above Pearson correlation analysis, though in a PC1-PC2 biplot representing lower variance percentage (67.2%).

4.5. Radiological risk assessment

As aforementioned, human consumption of seaweed has increased significantly over the past decade. Algae are introduced into the human diet either by direct or indirect intake through the trophic chain. Other ways of influencing human could also be considered due

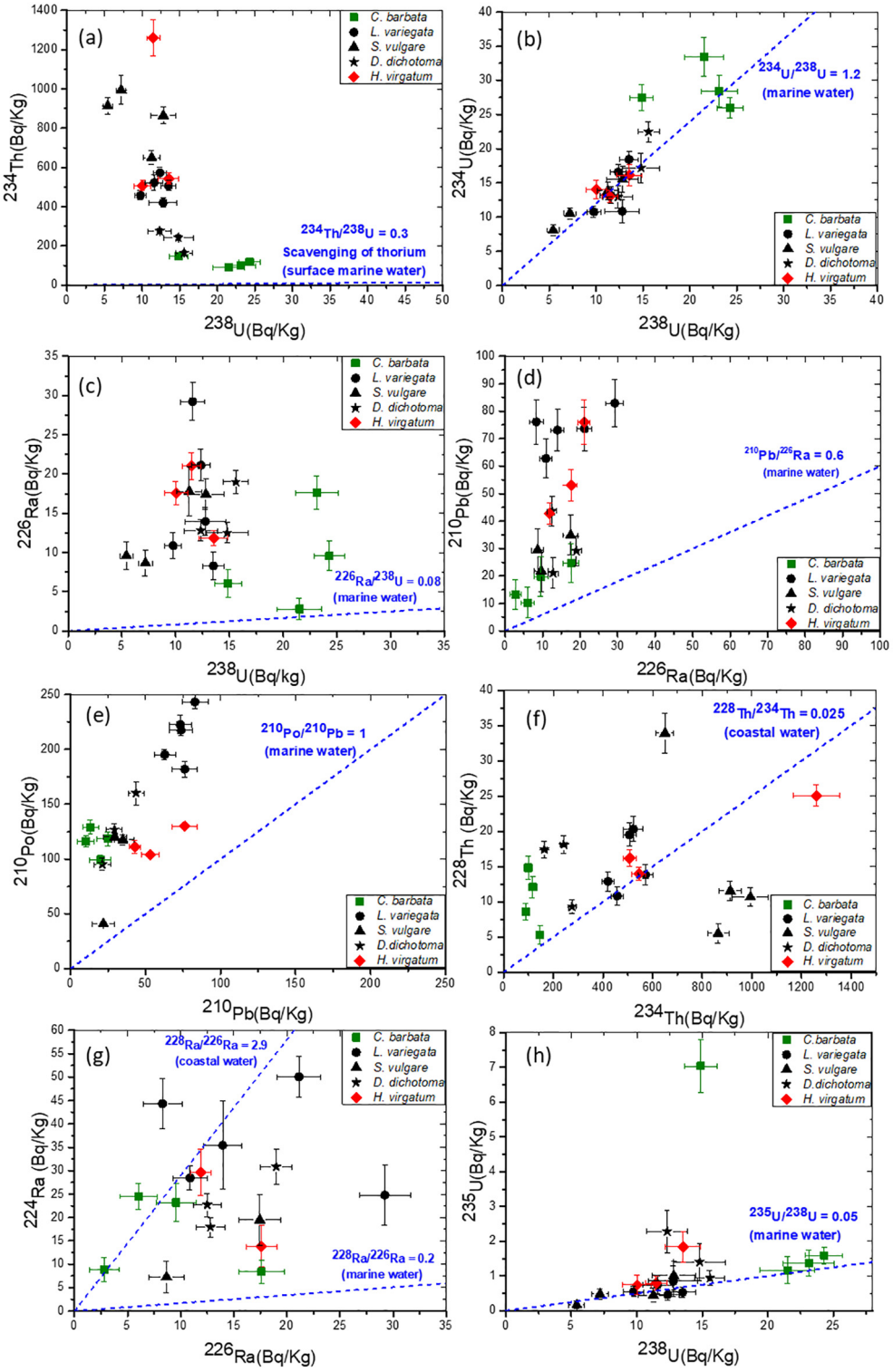

Fig. 2. Ratios between $^{234}Th/^{238}U$, $^{234}U/^{238}U$, $^{226}Ra/^{238}U$, $^{210}Pb/^{226}Ra$, $^{210}Po/^{210}Pb$, $^{228}Th/^{234}Th$, $^{224}Ra/^{226}Ra$ and $^{235}U/^{238}U$ for algae samples from January 2017 to May 2017. The dashed blue line shows the radioisotope equilibrium in marine water.

to seaweeds are used as, food products, animal feed ingredients, for extraction of carbohydrates, fertilizers or pharmaceutical and nutraceutical applications. Seaweeds, besides being rich in nutrients, can accumulate several compounds such as potentially toxic trace metals or radionuclides from the surrounding environment, which can be harmful when they are consumed by humans (Tiwari and Troy, 2015). Consequently, it is important to calculate a dose of activity concentration for radioisotopes by ingestion. This dose is known as the annual committed effective dose and was calculated according to the following equation (Khan and Wesley, 2016; Kim et al., 2017):

$$ACED = MF \times e(T) \times A \times I \quad (1)$$

where for each radionuclide, ACED is the annual committed effective dose for an individual, *MF* is a weighted factor to account for the delay between seafood catch and consumption, *e(T)* is the dose conversion

Table 4
Ratio between mean activity concentration of $^{234}Th/^{238}U$, $^{234}U/^{238}U$, $^{226}Ra/^{238}U$, $^{210}Pb/^{226}Ra$, $^{210}Po/^{210}Pb$, $^{224}Ra/^{228}Th$, $^{228}Th/^{234}Th$, $^{224}Ra/^{226}Ra$ and $^{235}U/^{238}U$ in green, brown and red algae of Las Canteras beach. Mean represents the average between the brown algae.

Ratio	Green	Brown				Red
	GC	BL	BS	BD	BMean	RH
$^{234}Th/^{238}U$	5.8 ± 0.7	42 ± 5	108 ± 14	16 ± 2	57 ± 7	67 ± 8
$^{234}U/^{238}U$	1.42 ± 0.12	1.16 ± 0.12	1.35 ± 0.17	1.22 ± 0.15	1.24 ± 0.14	1.24 ± 0.14
$^{226}Ra/^{238}U$	0.42 ± 0.09	1.4 ± 0.2	1.5 ± 0.3	1.03 ± 0.15	1.3 ± 0.2	1.49 ± 0.18
$^{210}Pb/^{226}Ra$	2.5 ± 1.3	5.3 ± 1.0	2.6 ± 0.8	2.9 ± 0.5	3.7 ± 0.8	3.4 ± 0.4
$^{210}Po/^{210}Pb$	8 ± 3	2.9 ± 0.3	3.1 ± 0.8	4.2 ± 0.6	3.3 ± 0.6	2.1 ± 0.2
$^{224}Ra/^{228}Th$	2.0 ± 0.5	2.5 ± 0.5	2.1 ± 0.8	1.7 ± 0.2	2.2 ± 0.5	1.5 ± 0.3
$^{228}Th/^{234}Th$	0.096 ± 0.016	0.031 ± 0.004	0.020 ± 0.003	0.072 ± 0.00	0.038 ± 0.004	0.026 ± 0.002
$^{224}Ra/^{226}Ra$	3 ± 1	2.7 ± 0.6	1.0 ± 0.4	1.6 ± 0.2	2.1 ± 0.5	1.6 ± 0.4
$^{235}U/^{238}U$	0.16 ± 0.03	0.053 ± 0.019	0.05 ± 0.02	0.11 ± 0.03	0.07 ± 0.02	0.09 ± 0.03

Table 5
Pearson correlation analysis between radionuclides of the algae from Las Canteras beach (correlation coefficient is shown at the bottom left diagonal and p-value cursive at the top of diagonal).

	^{238}U	^{234}U	^{235}U	^{210}Po	^{234}Th	^{226}Ra	^{210}Pb	^{228}Th	^{224}Ra	^{40}K
^{238}U	**1.00**	*0.00**	*0.29*	*0.95*	*0.00*	*0.47*	*0.15*	*0.59*	*0.45*	*0.06*
^{234}U	0.88	**1.00**	*0.05*	*0.76*	*0.00*	*0.17*	*0.03*	*0.34*	*0.36*	*0.15*
^{235}U	0.26	0.46	**1.00**	*0.62*	*0.08*	*0.15*	*0.06*	*0.08*	*0.72*	*0.58*
^{210}Po	0.01	−0.08	−0.12	**1.00**	*0.63*	*0.20*	*0.00*	*0.73*	*0.01*	*0.03*
^{234}Th	−0.72	−0.71	−0.42	−0.12	**1.00**	*0.26*	*0.11*	*0.28*	*0.78*	*0.19*
^{226}Ra	−0.18	−0.33	−0.34	0.31	0.27	**1.00**	*0.01*	*0.03*	*0.43*	*0.23*
^{210}Pb	−0.35	−0.49	−0.44	0.74	0.38	0.56	**1.00**	*0.09*	*0.01*	*0.05*
^{228}Th	−0.13	−0.23	−0.41	−0.09	0.26	0.50	0.40	**1.00**	*0.22*	*0.33*
^{224}Ra	−0.20	−0.24	−0.10	0.60	0.08	0.21	0.65	0.33	**1.00**	*0.10*
^{40}K	−0.44	−0.34	−0.14	−0.50	0.32	−0.29	−0.46	0.24	−0.43	**1.00**

* p-value = 0.00 corresponds to $p < 0.005$ (strong correlation).

(1.2, 0.69, 0.28, 3.4×10^{-3}, 4.9×10^{-2}, 4.5×10^{-2} and 6.2×10^{-3} μSv/Bq for ^{210}Po, ^{210}Pb, ^{226}Ra, ^{234}Th, ^{234}U, ^{238}U and ^{40}K respectively; UNSCEAR, 2000, 2008, 2016), *A* is the activity concentration in Bq/kg (for this dosimetry study, FW was considered), and *I* is the annual intake rate of macroalgae (kg/y) per individual. For the calculation of *MF*, it was considered that the delay that may exist in the processing and distribution of fish products from capture to consumption is 93 days for ^{210}Po, slightly less than its half-life (138.37 days) as it is recommended by UNSCEAR (2000). If for this same radionuclide the delay time were considered lower, for example 7 days (more realistic for the case of fresh algae consumption), this factor would be increased, from the value considered of 0.6 to 1.0, and the intake dose would increase too. For ^{234}Th and ^{228}Th (with a half-life of 22.1 days and 1.91 years respectively), *MF* are 0.1 and 0.9 for 93 days, or 0.8 and 1.0 for 7 days. Finally, *MF* is considered unity for ^{210}Pb, ^{226}Ra, ^{234}U, ^{238}U and ^{40}K due to its longer half-life.

In this work, doses were calculated (Table 7) assuming an intake of 10 kg/y FW, which is slightly lower than the safe recommendations for the intake of seaweed (i.e. 11–18 kg/y FW) (Tiwari and Troy, 2015). This considered value was even lower than that for Asian countries where the consumption of marine food, and more specifically algae, in the diet is more common, with an intake of 11 kg/y (Kim et al., 2017). Annual effective dose per adult individual considering all radionuclides involving algae ingestion ranged from 126 ± 7 to 423 ± 16 μSv/y (for 93 days delay), or 180 ± 7 to 605 ± 19 μSv/y when 7 days delay were taking account (Table 7). So we could see that the maximum ACED value was for *H. virgatum* and the minimum was for *S. vulgare*. Although, in general, ^{210}Po contributes most to the dose, the effective

Table 6
Factor loadings of radiological variables on four significant principal components for algae samples. Percentage of variance explained by each principal component and their cumulative percentage of total variance are also given.

Variables	PC1	PC2	PC3	PC4
^{238}U	0.55	0.09	−0.16	0.37
^{234}U	0.55	−0.01	−0.14	0.42
^{210}Po	−0.05	0.61	0.55	0.36
^{234}Th	−0.50	−0.07	−0.57	0.58
^{210}Pb	−0.30	0.56	−0.10	0.07
^{40}K	−0.22	−0.54	0.57	0.46
% of variance	48.7	35.8	8.1	4.4
Cumulative %	48.7	84.5	92.6	97.0

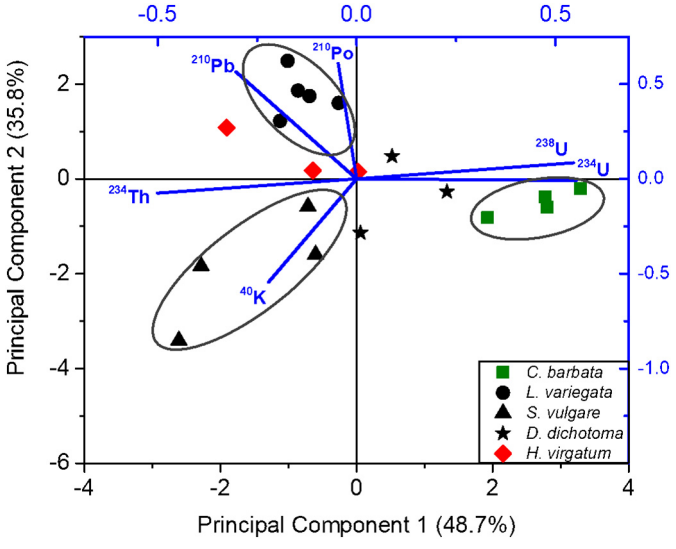

Fig. 3. Biplot of principal component (PC1 and PC2) scores based on observations for each alga specie (black axes). Radiological variables are plotted in blue axes. Numbers in brackets are the percentage of variance associated with each PC-axis, and ovals denote the clustering of algae samples.

Table 7
Annual effective dose per adult consumer by ingestion of radionuclides from seaweed (μSv/y).

	Green	Brown				Red
Radionuclide	**GC**	**BL**	**BS**	**BD**	**BMean**	**RH**
^{238}U	1.84 ± 0.15	0.98 ± 0.09	0.52 ± 0.06	1.82 ± 0.19	1.03 ± 0.11	1.62 ± 0.14
^{234}U	2.7 ± 0.2	1.22 ± 0.11	0.74 ± 0.07	2.5 ± 0.2	1.37 ± 0.13	2.12 ± 0.18
^{210}Po	160 ± 8	276 ± 8	77 ± 3	265 ± 15	219 ± 8	262 ± 8
^{226}Ra	5 ± 1	8.2 ± 1	4.7 ± 0.8	11.7 ± 1.1	7.9 ± 0.9	15.2 ± 1.2
^{210}Pb	23 ± 8	91 ± 10	23 ± 6	63 ± 10	65 ± 9	130 ± 14
^{228}Th	1.32 ± 0.18	1.78 ± 0.18	1.34 ± 0.14	2.8 ± 0.2	1.9 ± 0.17	4 ± 0.3
^{40}K	11 ± 0.5	7.9 ± 0.4	17.7 ± 0.8	19.3 ± 0.9	14 ± 0.7	6.4 ± 0.4
Total (93 days delay)	**205 ± 11**	**388 ± 13**	**126 ± 7**	**366 ± 18**	**310 ± 12**	**423 ± 16**
Total (7 days delay)	**312 ± 15**	**574 ± 17**	**180 ± 7**	**540 ± 30**	**458 ± 17**	**605 ± 19**

doses of ^{210}Pb for *H. virgatum* and L. *variegata* were also high. Finally, if we compare ACED values obtained in this work with representative doses due to other seafood (68.2, 181.5 and 381.8 μSv/y for fish, crustaceans and molluscs, respectively) (Livingston, 2004), one can see that most algae (except to *S. vulgare*) sampled had doses higher than doses due to fish and crustaceans, and even higher than of molluscs for the case of *H. virgatum*. Finally, if the 7 days delay is assumed doses due to algae consumption are still higher.

5. Conclusions

In this study, a baseline for natural radioactivity in five globally common seaweed species collected in arrivals on the Canary coast was established. The radionuclide accumulation power of different algae species, U and Th series ratios and internal doses were also determined. Besides, since these algae are not exclusive to the study region, this radiological characterization could be of more general interest, and useful for valorising these marine products in the future.

A tendency to accumulate radionuclides by seaweed has been proven, being more pronounced for reactive-particle radionuclides (^{210}Po, ^{234}Th, ^{228}Th and ^{210}Pb) than for conservative ones (^{40}K and the uranium isotopes). Brown and red algae exhibited CF values for particle-reactive radionuclides one or two orders higher than those recommended by the IAEA (2014) for macroalgae. Also, higher values for disequilibrium ratios were found for ^{234}Th/^{238}U and ^{210}Po/^{210}Pb. On the other hand, the PCA led to three differentiated clusters corresponding to three different algae species, *L. variegate, C. barbata and S. vulgare* that are characterized respectively by its predilection for ^{210}Pb and ^{210}Po (the former), for uranium radioisotopes (the second) and for ^{40}K and ^{234}Th (the latter).

Annual effective dose per adult individual reached values higher than the maximum values reported for other seafood in the literature, being ^{210}Po the radionuclide which most contributes to the ACED (60% – 85%). For this reason, a radiological assessment should be performed before the use of these algae for human consumption.

Finally, the radionuclide-accumulating power of algae is useful as an indicator of the surrounding radiological environment, and also as tracer of different environmental processes. This ability to concentrate the natural radionuclides studied in this paper could also be helpful to remediate waters contaminated with radionuclides by NORM industries.

Acknowledgement

Part of this work was financed by the Spanish Nuclear Safety Council (CSN) through a grant from its R&D programme for 2009.

References

Al-Masri, M.S., Mamish, S., Budier, Y., 2003. Radionuclides and trace metals in eastern Mediterranean Sea algae. J. Environ. Radioact. 67, 157–168. https://doi.org/10.1016/S0265-931X(02)00177-7.

Al-Qaradawi, I., Abdel-Moati, M., Al-Yafei, M.A., Al-Ansari, E., Al-Maslamani, I., Holm, E., Al-Shaikh, I., Mauring, A., Pinto, P.V., Abdulmalik, D., Amir, A., Miller, M., Yigiterhan, O., Persson, B., 2015. Radioactivity levels in the marine environment along the Exclusive Economic Zone (EEZ) of Qatar. Mar. Pollut. Bull. 90, 323–329. https://doi.org/10.1016/j.marpolbul.2014.10.021.

Arnedo, M.A., Tejera, A., Rubiano, J.G., Alonso, H., Gil, J.M., Rodríguez, R., Martel, P., 2013. Natural radioactivity measurements of beach sands in gran Canaria, Canary Islands (Spain). Radiat. Prot. Dosim. 156, 75–86. https://doi.org/10.1093/rpd/nct044.

Arnedo, M.A., Rubiano, J.G., Alonso, H., Tejera, A., González, A., González, J., Gil, J.M., Rodríguez, R., Martel, P., Bolivar, J.P., 2017. Mapping natural radioactivity of soils in the eastern Canary Islands. J. Environ. Radioact. 166, 242–258. https://doi.org/10.1016/j.jenvrad.2016.07.010.

Blasco, M., Gázquez, M.J., Pérez-Moreno, S.M., Grande, J.A., Valente, T., Santisteban, M., de la Torre, M.L., Bolívar, J.P., 2016. Polonium behaviour in reservoirs potentially affected by acid mine drainage (AMD) in the Iberian Pyrite Belt (SW of Spain). J. Environ. Radioact. 152, 60–69. https://doi.org/10.1016/j.jenvrad.2015.11.008.

Bolívar, J.P., Garcia-Tenorio, R., Vaca, F., 2000. Radioecological study of an estuarine system located in the south of Spain. Water Res. 34, 2941–2950. https://doi.org/10.1016/S0043-1354(99)00370-X.

Boryło, A., Skwarzec, B., 2014. Activity disequilibrium between ^{234}U and ^{238}U isotopes in natural environment. J. Radioanal. Nucl. Chem. 300, 719–727. https://doi.org/10.1007/s10967-014-3001-9.

Bronson, F., 2003. Validation of the accuracy of the LabSOCS software for mathematical efficiency calibration of Ge detectors for typical laboratory samples. J. Radioanal. Nucl. Chem. 255 (1), 137–141. https://doi.org/10.1023/A:1022248318741.

Burger, J., Gochfeld, M., Kosson, D.S., Powers, C.W., Jewett, S., Friendlander, B., Chenelot, H., Volz, C.D., Jeitnet, C., 2006. Radionuclides in marine macroalgae from Amchitka and Kiska Islands in the Aleutians: establishing a baseline for future biomonitoring. J. Environ. Radioact. 91, 27–40. https://doi.org/10.1016/j.jenvrad.2006.08.003.

Chakraborty, S., Bhattacharya, T., Singh, G., Maity, J.P., 2014. Benthic macroalgae as biological indicators of heavy metal pollution in the marine environments: a biomonitoring approach for pollution assessment. Ecotoxicol. Environ. Saf. 100, 61–68. https://doi.org/10.1016/j.ecoenv.2013.12.003.

Cochran, J.K., Thomas, M.-V., Dornblaser, M.M., Hirschberg, D., Livingston, H.D., Buesseler, K.O., 1990. ^{210}Pb scavenging in the North Atlantic and North Pacific Oceans. Earth Planet. Sci. Lett. 97, 332–352. https://doi.org/10.1016/0012-821X(90)90050-8.

El Samad, O., Aoun, M., Nsouli, B., Khalaf, G., Hamze, M., 2014. Investigation of the radiological impact on the coastal environment surrounding a fertilizer plant. J. Environ. Radioact. 133, 69–74. https://doi.org/10.1016/j.jenvrad.2013.05.009.

Espino, F., Boyra, A., Tuya, F., Haroun, R., 2007. Guía Visual de Especies Marinas de Canarias. second ed. Oceanografica, Las Palmas de Gran Canaria.

Faganeli, J., Falnoga, I., Benedik, L., Jeran, Z., Klun, K., 2017. Accumulation of ^{210}Po in coastal waters (Gulf of Trieste, Northern Adriatic Sea). J. Environ. Radioact. 174, 38–44. https://doi.org/10.1016/j.jenvrad.2016.07.018.

FAO, 2018. The State of World Fisheries and Aquaculture 2018 - Meeting the Sustainable Development Goals (Rome).

G. Guerra, J., G. Rubiano, J., Winter, G., G. Guerra, A., Alonso, H., Arnedo, M.A., Tejera, A., Gil, J.M., Rodríguez, R., Martel, P., Bolivar, J.P., 2015. A simple methodology for characterization of germanium coaxial detectors by using Monte Carlo simulation and evolutionary algorithms. J. Environ. Radioact. 149, 8–18. https://doi.org/10.1016/j.jenvrad.2015.06.017.

G. Guerra, J., G. Rubiano, J., Winter, G., G. Guerra, A., Alonso, H., Arnedo, M.A., Tejera, A., Martel, P., Bolivar, J.P., 2017. Computational characterization of HPGe detectors usable for a wide variety of source geometries by using Monte Carlo simulation and a multi-objective evolutionary algorithm. Nucl. Inst. Methods Phys. Res. A 858, 113–122. https://doi.org/10.1016/j.nima.2017.02.087.

Gallardo, T., Bárbara, I., Afonso-Carrillo, J., Bermejo, R., Altamirano, M., Gómez Garreta, A., Barceló Martí, M.C., Rull Lluch, J., Ballesteros, E., De la Rosa, J., 2016. Nueva Lista Crítica de las Algas Bentónicas Marinas de España. ALGAS, Boletín Informativo de la Sociedad Española de Ficología.

Goddar, C.C., Jupp, B.P., 2002. The radionuclide content of seaweeds and seagrass around the coast of Oman and the United Arab Emirates. Mar. Pollut. Bull. 42, 1411–1416. https://doi.org/10.1016/S0025-326X(01)00218-1.

Guiry, M.D., 2018. In: Guiry, M.D., Guiry, G.M. (Eds.), AlgaeBase. World-wide electronic publication, National University of Ireland, Galway http://www.algaebase.org, Accessed date: 29 November 2018.

Hierro, A., Bolivar, J.P., Vaca, F., Borrego, J., 2012. Behavior of natural radionuclides in surficial sediments from an estuary impacted by acid mine discharge and industrial

effluents in Southwest Spain. J. Environ. Radioact. 110, 13–23. https://doi.org/10.1016/j.jenvrad.2012.01.005.
Hosseini, A., Beresford, N.A., Brown, J.E., Jones, D.G., Phaneuf, M., Thørring, H., Yankovich, T., 2010. Background dose-rates to reference animals and plants arising from exposure to naturally occurring radionuclides in aquatic environments. J. Radiol. Prot. 30, 235–264. https://doi.org/10.1088/0952-4746/30/2/S03.
Hosseini, A., Brown, J.E., Gwynn, J.P., Dowdall, M., 2012. Review of research on impacts to biota of discharges of naturally occurring radionuclides in produced water to the marine environment. Sci. Total Environ. 438, 325–333. https://doi.org/10.1016/j.scitotenv.2012.08.047.
Hu, W., Chen, M., Yang, W., Zhang, R., Qiu, Y., Zheng, M., 2014. Enhanced particle scavenging in deep water of the Aleutian Basin revealed by ^{210}Po-^{210}Pb disequilibria. J. Geophys. Res. Oceans 119, 3235–3248. https://doi.org/10.1002/2014JC009819.
IAEA, 1992. Effects of Ionizing Radiation on Plants and Animals at Levels Implied by Current Radiation Protection Standards (Technical Reports Series 332).
IAEA, 2014. Sediment Distribution Coefficients and Concentration Factors for Biota in the Marine Environment (Technical Reports Series 422).
Inoue, M., Kofuji, H., Yamamoto, M., Komura, K., 2005. Seasonal variation of ^{228}Ra/^{226}Ra ratio in seaweed: implications for water circulation patterns in coastal areas of the Noto Peninsula, Japan. J. Environ. Radioact. 80, 341–355. https://doi.org/10.1016/j.jenvrad.2004.10.007.
Ishikawa, Y.Ã., Kagaya, H., Saga, K., 2004. Biomagnification of ^{7}Be, ^{234}Th, and ^{228}Ra in marine organisms near the northern Pacific coast of Japan. J. Environ. Radioact. 76, 103–112. https://doi.org/10.1016/j.jenvrad.2004.03.021.
Khan, M.F., Wesley, S.G., 2016. Baseline concentration of Polonium-210 (^{210}Po) in tuna fish. Mar. Pollut. Bull. 107, 379–382. https://doi.org/10.1016/j.marpolbul.2016.03.056.
Kim, S.H., Hong, G.H., Lee, H.M., Cho, B.E., 2017. ^{210}Po in the marine biota of Korean coastal waters and the effective dose from seafood consumption. J. Environ. Radioact. 174, 30–37. https://doi.org/10.1016/j.jenvrad.2016.11.001.
Kohler, U., Luniak, M., 2005. Data inspection using biplots. Stata J. 5, 208–223. https://doi.org/10.1177/1536867X0500500206.
Livingston, H.D., 2004. Radioactivity in the Environment: Marine Radioactivity. First. ed. Elsevier Ltd, Oxford.
Mat Çatal, E., Uğur, A., Özden, B., Filizok, I., 2012. ^{210}Po and ^{210}Pb variations in fish species from the Aegean Sea and the contribution of ^{210}Po to the radiation dose. Mar. Pollut. Bull. 64, 801–806. https://doi.org/10.1016/j.marpolbul.2012.01.016.
Matiatos, I., Alexopoulos, A., Godelitsas, A., 2014. Multivariate statistical analysis of the hydrogeochemical and isotopic composition of the groundwater resources in northeastern Peloponnesus (Greece). Sci. Total Environ. 476–477, 577–590. https://doi.org/10.1016/j.scitotenv.2014.01.042.
McDonald, P., Cook, G.T., Baxter, M.S., 1992. Natural and anthropogenuc radioactivity in coastal regions of the UK. Radiat. Prot. Dosim. 45, 707–710. https://doi.org/10.1007/978-94-011-3686-0_35.
Medina Santamaría, R., Batón Meira, S., Cánovas Losada, V., Torres Freyermuth, A., Luque Escalona, Á., Alonso Bilbao, I., Sánchez Pérez, I., Ortega García, A., Rodríguez Valido, S., Martín García, J.A., García Jiménez, P., Santos Facundo, F., Bilbao Siero, A., López Menviel, F., Cabanillas Terán, N., Bustos León, R., Sollheim González, C., López Caballero, Y., García Fernández, Y., 2006. Estudio integral de la playa de Las Canteras. Inf. Técnico Para la Dir. Gen. Costas. vol. 736.
Montaña, M., Fons, J., Corbacho, J.A., Camacho, A., Zapata-García, D., Guillén, J., Serrano, I., Tent, J., 2013. A comparative experimental study of gross alpha methods in natural waters. J. Environ. Radioact. 118, 1–8. https://doi.org/10.1016/j.jenvrad.2012.10.009.
Osvath, I., Tarjan, S., Pitois, A., Groening, M., Osborn, D., 2016. IAEA's ALMERA network: supporting the quality of environmental radioactivity measurements. Appl. Radiat. Isot. 109, 90–95. https://doi.org/10.1016/j.apradiso.2015.12.062.
Outola, I., Filliben, J., Inn, K.G.W., La Rosa, J., McMahon, C.A., Peck, G.A., Twining, J., Tims, S.G., Fifield, L.K., Smedley, P., Antón, M.P., Gascó, C., Povinec, P., Pham, M.K., Raaum, A., Wei, H.-J., Krijger, G.C., Bouisset, P., Litherland, A.E., Kieser, W.E., Betti, M., delas Heras L., Aldave, Hong, G.H., Holm, E., Skipperud, L., Harms, A.V., Arinc, A., Youngman, M., Arnold, D., Wershofen, H., Sill, D.S., Bohrer, S., Dahlgaard, H., Croudace, I.W., Warwick, P.E., Ikäheimonen, T.K., Klemola, S., Vakulovsky, S.M., Sanchez-Cabeza, J.A., 2006. Characterization of the NIST seaweed Standard Reference Material. Appl. Radiat. Isot. 64, 1242–1247. https://doi.org/10.1016/j.apradiso.2006.02.029.
Pentreath, J.R., 1988. Radionuclides in the aquatic environment. In: Harley, J.H., Schmidt, G.D., Silini, G. (Eds.), Radionuclides in the Food Chain. Springer-Verlag, New York, pp. 99–119.
Pham, M.K., Benmansour, M., Carvalho, F.P., Chamizo, E., Degering, D., Engeler, C., Gascó, C., Gwynn, J.P., Harms, A.V., Hrnecek, E., Ibanez, F.L., Ilchmann, C., Ikaheimonen, T., Kanisch, G., Kloster, M., Llaurado, M., Mauring, A., Møller, B., Morimoto, T., Nielsen, S.P., Nies, H., Norrlid, L.D.R., Pettersson, H.B.L., Povinec, P.P., Rieth, U., Samuelsson, C., Schikowski, J., Šilobritiene, B.V., Smedley, P.A., Suplinska, M., Vartti, V.-P., Vasileva, E., Wong, J., Zalewska, T., Zhou, W., 2014. Certified Reference Material IAEA-446 for radionuclides in Baltic. Appl. Radiat. Isot. 87, 468–474. https://doi.org/10.1016/j.apradiso.2013.11.013.
Portillo Hahnefeld, E., 2008. Arribazones de Algas y Plantas Marinas en Gran Canarias: Características, Gestión y Posibles Usos. First. ed. Daute Diseño, S.L., Santa Lucía-Las Palmas.
Praveen Pole, R.P., Feroz Khan, M., Godwin Wesley, S., 2017. Occurrence of ^{210}Po in marine macroalgae inhabiting a coastal nuclear zone, southeast coast of India. J. Environ. Radioact. 169–170, 122–130. https://doi.org/10.1016/j.jenvrad.2017.01.013.
Rajacic, M.M., Todorovic, D.J., Nikolic, J.D.K., Puzovic, J.M., 2017. The impact of the Solar magnetic field on ^{7}Be activity concentration in aerosols. Appl. Radiat. Isot. 125, 27–29. https://doi.org/10.1016/j.apradiso.2017.04.008.
Sá, S., Bastos-Santos, J., Araújo, H., Ferreira, M., Duro, V., Alves, F., Panta-Ferreira, B., Nicolau, L., Eira, C., Vingada, J., 2016. Spatial distribution of floating marine debris in offshore continental Portuguese waters. Mar. Pollut. Bull. 104, 269–278. https://doi.org/10.1016/j.marpolbul.2016.01.011.
Sakamoto, N., Kano, N., Imaizumi, H., 2008. Determination of rare earth elements, thorium and uranium in seaweed samples on the coast in Niigata Prefecture by inductively coupled plasma mass spectrometry. Appl. Geochem. 23, 2955–2960. https://doi.org/10.1016/j.apgeochem.2008.04.011.
Shakhashiro, A., Tarjan, S., Ceccatelli, A., Kis-Benedek, G., Betti, M., 2012. IAEA447: a new certified reference material for environmental radioactivity measurements. Appl. Radiat. Isot. 70, 1632–1643. https://doi.org/10.1016/j.apradiso.2012.03.024.
Sirelkhatim, D.A., Sam, A.K., Hassona, R.K., 2008. Distribution of ^{226}Ra – ^{210}Pb – ^{210}Po in marine biota and surface sediments of the Red Sea, Sudan. J. Environ. Radioact. 99, 1825–1828. https://doi.org/10.1016/j.jenvrad.2008.07.008.
Strezov, A., Nonova, T., 2009. Influence of macroalgal diversity on accumulation of radionuclides and heavy metals in Bulgarian Black Sea ecosystems. J. Environ. Radioact. 100, 144–150. https://doi.org/10.1016/j.jenvrad.2008.09.007.
Su, K., Du, J., Baskaran, M., Zhang, J., 2017. ^{210}Po and ^{210}Pb disequilibrium at the PN section in the East China Sea. J. Environ. Radioact. 174, 54–65. https://doi.org/10.1016/j.jenvrad.2016.07.031.
Suriyanarayanan, S., Brahmanandhan, G.M., Malathi, J., Ravi Kumar, S., Masilamani, V., Shahul Hameed, P., Selvasekarapandian, S., 2007. Studies on the distribution of ^{210}Po and ^{210}Pb in the ecosystem of Point Calimere Coast (Palk Strait), India. J. Environ. Radioact. 99, 766–771. https://doi.org/10.1016/j.jenvrad.2007.10.003.
Tang, Y., Stewart, G., Lam, P.J., Rigaud, S., Church, T., 2017. The influence of particle concentration and composition on the fractionation of ^{210}Po and ^{210}Pb along the North Atlantic GEOTRACES transect GA03. Deep-Sea Res. I 128, 42–54. https://doi.org/10.1016/j.dsr.2017.09.001.
Theng, T.L., Abd, C., Mohamed, R., 2005. Activities of ^{210}Po and ^{210}Pb in the water column at Kuala Selangor, Malaysia. J. Environ. Radioact. 80, 273–286. https://doi.org/10.1016/j.jenvrad.2004.10.004.
Thomson, R.E., Emery, W.J., 2014. Data analysis methods in physical oceanography. Climate Change 2013 - The Physical Science Basis, Third ed. Elsevier B.V., Waltham https://doi.org/10.1017/CBO9781107415324.004.
Tiwari, B.K., Troy, D.J., 2015. Seaweed Sustainability Food and Non-Food Applications. Academic Press. Elsevier, London.
Uddin, S., Aba, A., Bebhehani, M., 2015. Baseline concentration of ^{210}Po and ^{210}Pb in Sargassum from the northern Gulf. Mar. Pollut. Bull. 90, 330–333. https://doi.org/10.1016/j.marpolbul.2014.09.029.
Uddin, S., Fowler, S.W., Behbehani, M., Metian, M., 2017. Po bioaccumulation and trophic transfer in marine food chains in the northern Arabian Gulf. J. Environ. Radioact. 174, 23–29. https://doi.org/10.1016/j.jenvrad.2016.08.021.
UNSCEAR, 2000. Sources and effects of ionizing radiation. Report of the United Nations Scientific Committee on the Effects of Atomic Radiation to the General Assembly, with Scientific Annexes. United Nations, New York.
UNSCEAR, 2008. Sources and effects of ionizing radiation. Report of the United Nations Scientific Committee on the Effects of Atomic Radiation to the General Assembly, with Scientific Annexes. United Nations, New York.
UNSCEAR, 2016. Sources, effects and risks of ionizing radiation. Report of the United Nations Scientific Committee on the Effects of Atomic Radiation to the General Assembly, with Scientific Annexes. United Nations, New York.
van der Spiegel, M., Noordam, M.Y., van der Fels-Klerx, H.J., 2013. Safety of novel protein sources (insects, microalgae, seaweed, duckweed, and rapeseed) and legislative aspects for their application in food and feed production. Compr. Rev. Food Sci. Food Saf. 12, 662–678. https://doi.org/10.1111/1541-4337.12032.
Waples, J.T., Benitez-Nelson, C., Savoye, N., Rutgers van der Loeff, M., Baskaran, M., Gustafsson, Ö., 2006. An introduction to the application and future use of ^{234}Th in aquatic systems. Mar. Chem. 100, 166–189. https://doi.org/10.1016/j.marchem.2005.10.011.
Wei, C.L., Lin, S.Y., Sheu, D.D., Chou, W.C., Yi, M.C., Santschi, P.H., Wen, L.S., 2011. Particle-reactive radionuclides (^{234}Th, ^{210}Pb, ^{210}Po) as tracers for the estimation of export production in the South China Sea. Biogeosciences 8, 3793–3808. https://doi.org/10.5194/bg-8-3793-2011.
Yang, B., Ha, Y., Jin, J., 2015. Assessment of radiological risk for marine biota and human consumers of seafood in the coast of Qingdao, China. Chemosphere 135, 363–369. https://doi.org/10.1016/j.chemosphere.2015.04.097.